[9]Corsiglia, V. R., and Dunham, R. E., "Aircraft Wake Vortex Minimization by Use of Flaps," *NASA Symposium on Wake Vortex Minimization*, edited by A. Gessow, NASA SP-409, 1976, pp. 305–338.

[10]Leonard, A., "Numerical Simulation of Interacting, Three-Dimensional Vortex Filaments," *Proceeding of the 4th International Conference on Numerical Methods in Fluid Dynamics*, Boulder, CO, 1974, pp. 245–250; *Lecture Notes in Physics*, Vol. 35, Springer-Verlag, Berlin, 1975, pp. 245–250.

[11]Quackenbush, T. R., Bilanin, A. J., and McKillip, R. M., Jr., "Vortex Wake Control Via Smart Structures Technology," *Proceedings of the SPIE—The International Society for Optical Engineering*, Vol. 2721, SPIE, Bellingham, WA, 1996, pp. 78–92.

[12]Quackenbush, T. R., Bilanin, A. J., Batcho, P. F., McKillip, R. M., Jr., and Carpenter, B. F., "Implementation of Vortex Wake Control Using SMA-Actuated Devices," *Proceedings of the SPIE—The International Society for Optical Engineering*, Vol. 3044, SPIE, Bellingham, WA, 1997, pp. 134–146.

[13]Quackenbush, T. R., Batcho, P. F., Bilanin, A. J., and Carpenter, B. F., "Design, Fabrication, and Test Planning for an SMA-Actuated Vortex Wake Control System," *Proceedings of the SPIE—The International Society for Optical Engineering*, Vol. 3326, SPIE, Bellingham, WA, 1998, pp. 259–271.

[14]Klein, R., Majda, A. J., and Damodaran, K., "Simplified Equations for the Interaction of Nearly Parallel Vortex Filaments," *Journal of Fluid Mechanics*, Vol. 288, 1995, pp. 201–248.

[15]Jimenez, J., "Stability of a Pair of Co-Rotating Vortices," *Physics of Fluids*, Vol. 18, No. 11, 1975, pp. 1580, 1581.

[16]Schlichting, H., *Boundary-Layer Theory*, 7th ed., McGraw–Hill, New York, 1979, p. 638.

[17]Bristol, R. L., "Co-Operative Wake Vortex Instabilities," Ph.D. Dissertation, Univ. of California, Berkeley, CA, Dec. 2000.

[18]Ortega, J. M., "Stability Characteristics of Counter-Rotating Vortex Pairs in the Wakes of Triangular-Flapped Airfoils," Ph.D. Dissertation, Univ. of California, Berkeley, CA, May 2001.

A. Plotkin
Associate Editor

Influence of Boundary-Layer Thickness on Base Pressure and Vortex Shedding Frequency

A. Rowe,* A. L. A. Fry,* and F. Motallebi†
University of London,
London, England E1 4NS, United Kingdom

Nomenclature

C_{pb}	=	base pressure coefficient, $(p_b - p_s)/0.5\rho u^2$
f	=	vortex shedding frequency
H	=	boundary-layer shape factor, δ^*/θ
h	=	trailing-edge thickness
p_b	=	base pressure
p_s	=	static pressure at traverse position
Sr_h	=	Strouhal number, fh/u
u	=	freestream velocity
δ	=	boundary-layer thickness based on 99.5% of freestream velocity
δ^*	=	boundary-layer displacement thickness
θ	=	boundary-layer momentum thickness
ρ	=	density

Introduction

VORTEX shedding in the wake of bluff bodies is an important flow phenomenon. At subsonic and transonic speeds, it has long been recognized that the wake behind an isolated two-dimensional section with a blunt trailing edge may break into a vortex street. The direct result of this is an increase in drag, mainly as a result of reduced base pressure.[1–3] Several investigators have reported on the factors affecting the base drag and vortex shedding,[4–7] that is, base geometry, base bleed, state of the boundary layer at the trailing edge, etc. The objective of present study was to experimentally investigate the influence of the thickness of turbulent boundary layers upstream of trailing edge on the base pressure and vortex shedding frequency and for a given boundary-layer state (turbulent in this case) to determine the predominant parameters that affect the base drag and vortex shedding frequency. Further, unlike previous investigations,[1–7] where the change in the boundary-layer characteristics (thickness and/or state) has been brought about mainly as a result of change in Reynolds number and/or Mach number, in the present work the Reynolds number and Mach number were kept constant and the change in the boundary-layer thickness has been brought about by introducing roughness elements.

Experimental Setup and Procedures

The experiments were conducted at zero pressure gradient and at two speeds. The low-speed experiments (nominal freestream velocity of 23 m/s) were performed in a closed-circuit wind tunnel with a 1.0×0.77 m rectangular section of length 2.30 m. The model (Fig. 1) consisted of a flat plate, 0.05 m thick, 0.77 m wide, and 1.0 m long with an elliptical leading edge and a square cut trailing edge. The nominal freestream Reynolds number based on the model's chord length was 1.7×10^6. To change the thickness of the boundary layer before the separation point, wires with different diameters were placed symmetrically at the end of the leading-edge curvature on both sides of the model. In total three wires with diameters of 1.62, 2.4, and 3.4 mm were used. The high-speed tests were conducted in a transonic wind tunnel with slotted walls. The tunnel has a working section of 8.9×16.5 cm. The tests were carried out at a freestream Mach number of 0.68. The freestream Reynolds number based on the chord of the model was about 2.15×10^6. The model used in high-speed tests was essentially similar in design with that of the low-speed test and had an elliptic leading edge followed by a straight rectangular section, as shown in Fig. 1. The high-speed experiments were carried out for only two boundary-layer thicknesses (with and without roughness element).

Measurement of the boundary-layer profiles was made at a point upstream of the trailing edge (see Tables 1 and 2), where the surface static pressure on the model begins to decrease as the blunt trailing edge is approached. The total pressure across the boundary layer was measured using flat-ended pitot probes. The static pressure across the boundary layer was assumed to be constant and equal to the pressure recorded by the surface pressure tap. The physical boundary-layer thickness was defined as the distance perpendicular to the model surface where the velocity was approximately 0.995 of the local freestream velocity. Tables 1 and 2 give the details of the boundary-layer parameters determined from the experimental surveys of the boundary layer. No corrections were made to account for the displacement effects of the pitot tube. Temperature compensated piezoresistive pressure sensors (Scanivalve digital sensor arrays, Model DSA 3017) were used for pressure measurements. The low-pressure model (pressure range ±2.5 kPa) had an accuracy of ±0.3% and the high-pressure model (pressure range −100–690 kPa) had an accuracy of ±0.08%. The measurement of the vortex shedding frequency was carried out by placing a hot-wire probe behind the trailing edge of the model. The location of the probe tip was slightly above the model surface (this position was slightly different for each test case to get the best periodic signals, but was within the 10% of the base height) at a distance of approximately half of the base height behind the trailing and in the center-span plane of the models. The

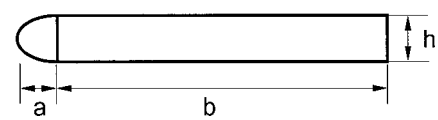

Fig. 1 Schematic profile of experimental model; low-speed model: $a = 10$, $b = 90$, and $h = 5$; high-speed model: $a = 2.5$, $b = 10$, and $h = 1$ (dimensions are in centimeters).

Received 2 February 2000; revision received 27 November 2000; accepted for publication 28 November 2000. Copyright © 2001 by the American Institute of Aeronautics and Astronautics, Inc. All rights reserved.

*Student, Department of Engineering, Queen Mary.
†Lecturer, Department of Engineering, Queen Mary.

output signal of the hot wire was then fed to a National Instrument Data Acquisition card (Model PCI-6071E) and processed in real time. From spectral analysis of the signal, the shedding frequency of vortices was determined. The maximum uncertainty of the vortex shedding frequency was within ±0.6% (low-speed experiments) and ±0.9% (high-speed experiments). Two pressure taps drilled symmetrically across the trailing-edge thickness were used to measure the base pressure p_b. The same reading may be obtained from a pitot tube with its mouth placed immediately behind the face of trailing edge. When the pitot tube is traversed in the spanwise direction behind the trailing edge, the variation of base pressure across the span may be obtained. From these measurements, it was found that the spanwise variation of base pressure was small over at least the mid-60% of the span (less than ±0.5% of p_b). Near the sidewalls, three-dimensional effects were present. These were probably caused by the interaction of the side wall boundary layer with model's surface boundary layer.

Results and Discussion

Tables 1 and 2 give the details of different boundary-layer parameters. In all cases in both sets of experiments, the boundary layer approaching the trailing edge was turbulent, and the effect of introducing wires was to change the boundary-layer thicknesses. The nondimensional displacement thickness $2\delta^*/(2\delta^* + h)$ represents the relative thickness of the boundary layers to their total effective separation distance. This parameter is used to show the effect of increasing the boundary-layer displacement thickness on the base pressure coefficient and Strouhal number incompressible flow (Fig. 2a) and compressible flow (Fig. 2b)]. As can be seen, in both cases the effect of increasing the boundary-layer thickness was to increase the base pressure and to reduce the vortex shedding frequency. This may be explained as follows: As the displacement thickness of the boundary layer increases, it takes longer for the circulation fed by the upstream boundary layer on one side to be carried across the wake in a sufficient concentration to initiate the formation of a vortex on the opposite side (and, hence, the beginning of vortex shedding). Therefore, it seems that for a given state of boundary layers at the trailing edge this effective diffusion length, which depends solely on the effective distance between the two boundary layers, is the main factor in controlling the vortex shedding frequency and base drag. However, this argument cannot be used to explain the influence that the state of the boundary layer (laminar/turbulent) at the trailing edge has on the vortex shedding frequency and on the base drag. For example, although there do not appear to have been, for laminar flow, systematic studies of the effect of boundary-layer thickness on the shedding frequency and base drag, experimental data by Sieverding and Heinemann,[4,8] Cicatelli and Sieverding,[9] and Cicatelli[10] show that in the case of laminar boundary-layer flows the base drag is lower and vortex shedding is much higher than for the turbulent case. In fact, their experimental data suggest that, in the case of laminar flows, the Strouhal number is generally greater than 0.35 as compared with 0.2–0.25 for the corresponding turbulent case. This is despite the fact that, for laminar boundary layers, the displacement thickness, or the effective diffusion (or separation) distance between the two layers, is higher.[8] Therefore, it seems that, for a given state of boundary layers (turbulent-turbulent, laminar–laminar, or turbulent–laminar) at the trailing edge, increasing the effective distance between the two layers decreases the vortex shedding frequency with corresponding decrease in the base drag. However, this argument fails to explain the relationship between base drag and Strouhal number when the state of the two boundary layers at the trailing edge changes from turbulent–turbulent to laminar–laminar or to turbulent–laminar. This might be related to the variation of the base drag and vortex shedding frequency with the boundary-layer shape factor. Figure 3 shows the effect of variation of boundary-layer shape factor on the base pressure coefficient and on the Strouhal number. Figure 3 shows that the base pressure coefficient decreases with increasing boundary-layer shape factor with a corresponding increase in Strouhal number. Note that, for cases studied here, the rate of increase in momentum thickness was higher than the corresponding rate of increase in boundary-layer displacement thickness. From Fig. 3, it becomes clear that the increase in base drag cannot be attributed only to the increase in vortex shedding frequency (decrease in effective diffusion distance), but also to the intensity of vorticity within the inner part of the boundary layer (i.e., momentum thickness) and, therefore, shape factor. Note that in Fig. 3 the displacement thickness also changes, but for the reasons given earlier, that alone does not seem responsible for the change in behavior from the turbulent to the laminar boundary-layer case.

For laminar flows, the momentum thickness is lower compared to that of turbulent flows, with corresponding lower base drag. This

Table 1 Boundary-layer data for low-speed experiments, traverse location 20 mm upstream of trailing edge

Wire diameter k, mm	δ, mm	δ^*, mm	θ, mm	H	C_{pb}	S_h
0	14.410	1.829	1.333	1.372	−0.200	0.255
1.62	18.355	2.247	1.667	1.348	−0.197	0.238
2.40	23.341	2.503	1.890	1.325	−0.186	0.210
3.14	30.370	2.707	2.115	1.280	−0.172	0.194

Table 2 Boundary-layer data for high-speed experiments, traverse location 10 mm upstream of trailing edge

Wire diameter k, mm	δ, mm	δ^*, mm	θ, mm	H	C_{pb}	S_h
0	1.790	0.285	0.153	1.86	−0.638	0.230
0.5	5.440	0.644	0.430	1.50	−0.453	0.21

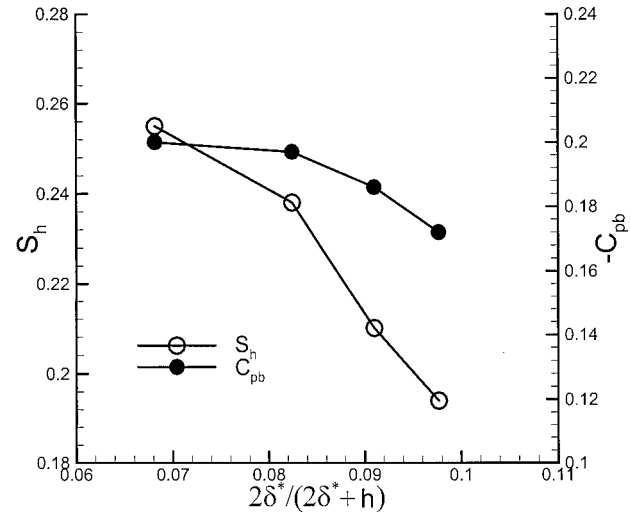

a) Low-speed experiments

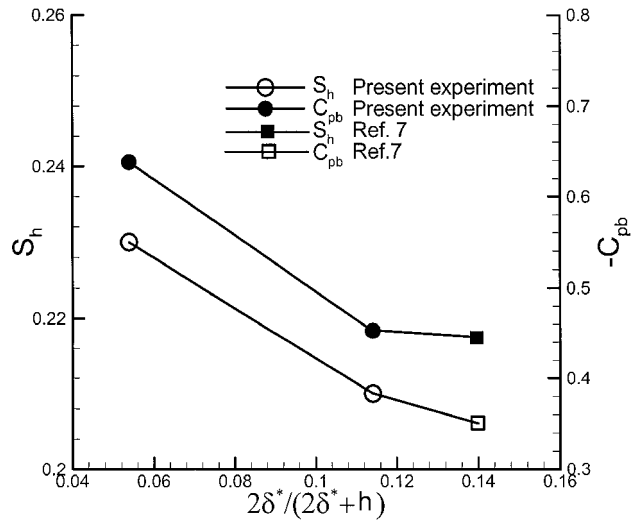

b) High-speed experiments

Fig. 2 Base pressure and Strouhal number variations with dimensionless displacement thickness.

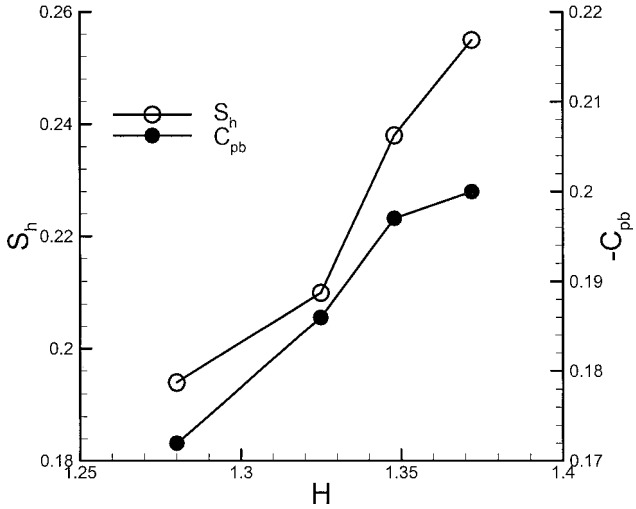

a) Low-speed experiments

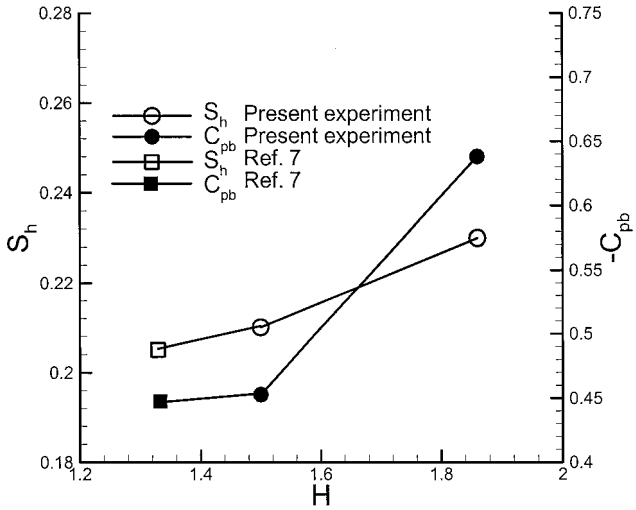

b) High-speed experiments

Fig. 3 Base pressure and Strouhal number variations with boundary-layer shape factor.

has been confirmed by calculations on both flat plates and turbine cascades.[11] The lower drag can also be explained by studying the vortex shedding mechanism.[12] For turbulent flows, as the boundary-layer thickness is decreased, the vorticity becomes less diffuse; therefore, it might take less time for the circulation to be carried across the wake in a sufficient strength to form a vortex of opposite sign to initiate the shedding of the vortices. This would result in a higher shedding frequency. This would imply that the rate of entrainment of fluid crossing from one side of the wake to the other increases as the boundary-layer thickness decreases. This in turn results into the shrinkage of the wake and lower base pressure (higher base drag). For laminar flows, the amount of circulation that needs to be carried across the wake to form a vortex of opposite sign is much less than the corresponding turbulent flow. The reduction in the required circulation to initiate the shedding of the vortices increases the vortex shedding frequency (despite higher effective diffusion length) and at the same time decreases the rate of entrainment of fluid crossing the wake, resulting in a lower base drag. These findings suggest that, whereas for a given state of the boundary layer at the trailing edge the effective diffusion distance between the boundary layers at the trailing edge controls the vortex shedding frequency, the shape factor is the determining parameter regardless of the boundary-layer state.

Conclusions

The results suggest that, at least for turbulent flows with zero streamwise pressure gradient, the relationship between the vortex shedding frequency and base drag with the boundary-layer thickness can be adequately explained by considering the variation of the boundary-layer shape factor. For both laminar and turbulent flows, this relationship can be described by considering the vortex formation mechanism through the strength of the vortices, effective diffusion length, and the entrainment rate of the fluid across the wake.

References

[1]Sieverding, C. H., Stanislas, M., and Snoek, J., "The Base Pressure Problem in Transonic Turbine Cascades," American Society of Mechanical Engineers, ASME Paper 79-GT-120, 1979.

[2]Xu, L., "The Base Pressure and Trailing Edge Loss of Transonic Blades," Ph.D. Dissertation, Dept. of Engineering, Univ. of Cambridge, Cambridge, England, U.K., Jan. 1985.

[3]Roshko, A., "The Drag and Shedding Frequency of 2-D Bluff Bodies," NACA TN 3169, 1954.

[4]Sieverding, C. H., and Heinemann, H., "The Influence of Boundary Layer State on Vortex Shedding from Flat Plates and Turbine Cascades," *Journal of Turbomachinery*, Vol. 112, April 1990, pp. 181–187.

[5]Edwards, S. J., Motallebi, F., and Norbury, J. F., "Base Pressure on a Blunt Base in Transonic Flow, Some Effects of Base Geometry and Bleed Air," American Society of Mechanical Engineers, ASME Paper 82-GT-317, 1982.

[6]Tanner, M., "Reducing of Base Drag," *Progress in Aerospace Sciences*, Vol. 16, No. 4, 1975, pp. 369–384.

[7]Motallebi, F., and Norbury, J. F., "The Effect of Base Bleed on Vortex Shedding and Base Pressure in Compressible Flow," *Journal of Fluid Mechanics*, Vol. 110, 1980, pp. 273–292.

[8]Sieverding, C. H., and Heinemann, H., "The Influence of Boundary Layer State on Vortex Shedding from Flat Plates and Turbine Cascades," American Society of Mechanical Engineers, ASME Paper 89-GT-296, 1989.

[9]Cicatelli, G., and Sieverding, C. H., "A Review of the Research on Unsteady Turbine Blade Wake Characteristics," *Loss Mechanisms and Unsteady Flows in Turbomachines*, AGARD PEP, May 1995, pp. 6-1–6-13.

[10]Cicatteli, G., "Time Varying Wake Flow Characteristics Behind Turbine Blade Wakes," Ph.D Dissertation, Dept. of Turbomachinery, von Kármán Inst., Universite Libre de Bruxelles, Brussels, July 1999.

[11]Deckers, M., "The Influence of Trailing Edge Coolant on the Loss of Transonic Turbine Blades," Ph.D. Dissertation, Dept. of Engineering, Univ. of Cambridge, Cambridge, England, U. K., June 1996.

[12]Gerrard, J. H., "The Mechanism of the Formation Region of Vortices Behind Bluff Bodies," *Journal of Fluid Mechanics*, Vol. 25, Pt. 2, 1966, pp. 401–413.

J. C. Hermanson
Associate Editor